Mark L. Winkler, MD • Douglas A. Ortendahl, PhD • Timothy C. Mills, PhD • Lawrence E. Crooks, PhD • Philip E. Sheldon, MS • Leon Kaufman, PhD • David M. Kramer, PhD

Characteristics of Partial Flip Angle and Gradient Reversal MR Imaging[1]

PARTIAL flip angle and gradient reversal magnetic resonance (MR) imaging have recently attracted a great deal of attention. Although these techniques are used together, they involve two independent physical phenomena, and each brings complementary contributions to the imaging process. Although partial flip MR imaging does not replace conventional spin-echo procedures, it has proved to be a powerful adjunctive tool for specific applications.

The ability to detect lesions with MR imaging is based on compositional differences among tissues and arises mostly from very simple effects. For a typical lesion, water content in the tissue increases, which results in correlated increases in relaxation times T1 and T2 and in hydrogen density, N(H). In a conventional spin-echo procedure, for any one set of imaging parameters (repetition time [TR]/echo time [TE]), the lengthening in T1 results in lowered signal intensity, while lengthened T2 and N(H) increase signal intensity. For medium to short TE values, there is a near cancellation of signal differences between the tissues, and contrast is poor. As TR lengthens, T1 effects become less important, and the effects of T2 and N(H) dominate (1). Lesions take on a characteristic "bright" or high-signal-intensity appearance.

In brain, cerebrospinal fluid has the MR properties of a lesion taken to extreme (Fig. 1). As a consequence, a very long TR or long TE is needed to render cerebrospinal fluid high in signal intensity, and all the strategies for obtaining this appearance have disadvantages. If a long TR value is used, the imaging time can be long, since a TR of 5 seconds or more is needed. These long TR images can be computed from two procedures with shorter TRs, but registration needs to be accurate between the two, and the time savings cannot be too great (maybe a factor of two) before the signal-to-noise ratio (S/N) degradation introduced by the calculations becomes excessive (2, 3). The alternative method of using long TE values at medium TR values incurs the penalty of loss of number of sections per unit time. It would be desirable to obtain the needed contrast with shorter TRs to reduce imaging times. To see how this can be achieved, we will discuss some basic aspects of MR imaging.

Index terms: Brain, MR studies, 10.1214 • Magnetic resonance (MR), image processing • Magnetic resonance (MR), physics • Magnetic resonance (MR), technology • State-of-art reviews

Radiology 1988; 166:17-26

BACK TO BASICS

In a conventional spin-echo image the magnetization vector is flipped by 90° onto the plane orthogonal to the main magnetic field. Because only the magnetization component on that plane provides signal, a 90° flip provides maximum signal, since all of the vector lies on that plane. But does a 90° flip provide maximum signal? Let us consider a flip of less than 90°, such as 45°. The first time the flip occurs, the magnetization vector projects only 70% on the orthogonal plane, while 70% remains on the equilibrium axis (Fig. 2). In imaging, data are accumulated many times. After the first time, for the 90° flip the magnetization has to recommence or "regrow" from zero, while for the 45° flip the regrowth starts at 70%. Given that successive data acquisitions occur at intervals of TR less than T1, even though the partial flip places less of the vector in the plane where it can provide signal, if a larger equilibrium magnetization is allowed for, the net effect is a larger vector on the signal-producing plane (Fig. 2). For a free induction decay and a TR that is not very short so that there is no residual transverse magnetization at the next subsequent RF pulse, the signal intensity (I) is

$$I = N(H)\frac{\sin\theta[1 - \exp(-TR/T1)]}{1 - \cos\theta \exp(-TR/T1)}. \quad (1)$$

Equation (1) is graphed in Figure 3 and has a maximum value of intensity at

$$\cos\theta = \exp(-TR/T1), \text{ or}$$
$$\theta = \arccos \exp(-TR/T1). \quad (2)$$

This effect is well known by MR spectroscopists, who take advantage of it to increase S/N. The angle θ at which the maximum signal occurs is called the Ernst angle, after Richard Ernst who described this effect (4), and is plotted as a function of TR for a T1 of 0.5 second in Figure 4. Compared with the signal from a 90° flip, the percentage increase in signal that results from a partial flip is

$$I(\theta)/I(90) = 100/\sqrt{[1 - \exp(-2TR/T1)]} = 100/\sin\theta. \quad (3)$$

From equation (2) we can see that for any one TR the Ernst angle is smaller (closer to zero), the longer the T1 is. From equation (3) we can see that this smaller angle results in a larger percentage of increase in signal.

[1] From the Department of Radiology, University of California, 400 Grandview Dr., South San Francisco, CA 94080 (M.L.W., D.A.O., T.C.M., L.E.C., P.E.S., L.K., D.M.K.) and Diasonics, Inc., Milpitas, California (D.M.K.). From the 1987 RSNA annual meeting. Received September 4, 1987; accepted October 13. **Address reprint requests to** M.L.W.

See also the articles by Brant-Zawadzki (pp. 1-10), Evens and Evens (pp. 27-30), and Heiken and Lee (pp. 11-16) in this issue.

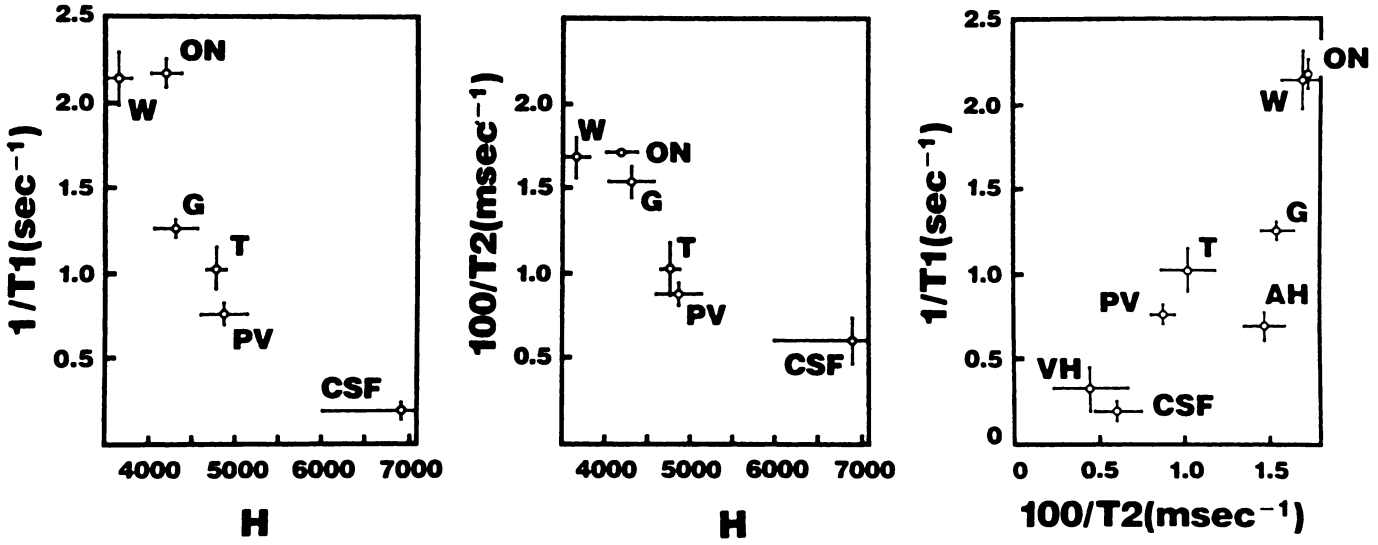

Figure 1. Correlation of tissue parameters in a patient with a primary brain tumor. For a typical lesion, water content in the tissue increases; this results in correlated increases in T1, T2, and N(H). This has important impact on the choice of imaging technique (1). The parameters are shown for white matter (*W*), optic nerve (*ON*), gray matter (*G*), tumor (*T*), periventricular edema (*PV*), aqueous humor (*AH*), vitreous humor (*VH*), and cerebrospinal fluid (*CSF*). Error bars are for single measurements. Optic nerve shows somewhat elevated density because of partial volume effects from fat, which raise average signal intensity. (Reprinted, with permission, from reference 1.)

These relationships lead to interesting results regarding the achievable S/N per unit time. For 90° flips, S/N per unit time is given by (5)

$$S/N \propto [1 - \exp(-TR/T1)]/\sqrt{TR}. \quad (4)$$

This single-section expression peaks at a TR of 1.25 × T1 and has a broad maximum of 90% of peak value of TRs between 0.6 and 2.6 × T1. For any one TE, the number of sections imaged is proportional to TR. Thus, to cover a given and large number of sections, the longer the TR, the fewer times that the imaging procedure has to be repeated, and in a fixed time the S/N goes up as $\sqrt{TR}$ increases. Thus, for multisection imaging of a large number of sections, equation (4) takes on the form

$$S/N \propto 1 - \exp(-TR/T1), \quad (5)$$

which means that from an S/N point of view the more sections needed, the better it is to lengthen TR. From equation (5), we also know that 90% of the achievable S/N is reached when TR equals 2.5 × T1.

The behavior of partial flip techniques is different. If we write equation (1) for the flip angle of maximum S/N (equation [2]), we obtain for the S/N per unit time the expression

$$S/N \propto \sqrt{\{[1 - \exp(-TR/T1)]/TR[1 + \exp(-TR/T1)]\}} = [\tan(\theta/2)]/\sqrt{TR}, \quad (6)$$

which has a maximum at TRs of 0; that is, to maximize S/N per unit time, partial flip techniques should be operated with very short TRs. But the variation of S/N with TR is very slow, and even when TR equals T1, the loss in S/N compared with TRs of 0 is about 13%. For a given large number of sections, the

$$S/N \propto \sqrt{\{[1 - \exp(-TR/T1)]/(1 + \exp(-TR/T1))\}} = \tan(\theta/2). \quad (7)$$

The product of this expression increases with TR but reaches 90% of maximum approximately when TR equals 2.5 × T1. Although it does not rapidly lose S/N per unit time as TR lengthens, partial flip MR imaging favors use of short TRs. Therefore, the partial flip technique is natural for use with three-dimensional imaging. For the 90° flip angle, the S/N per unit time always favors multisection imaging by large factors (6). With partial flips at the Ernst angle, S/N of the three-dimensional tech-

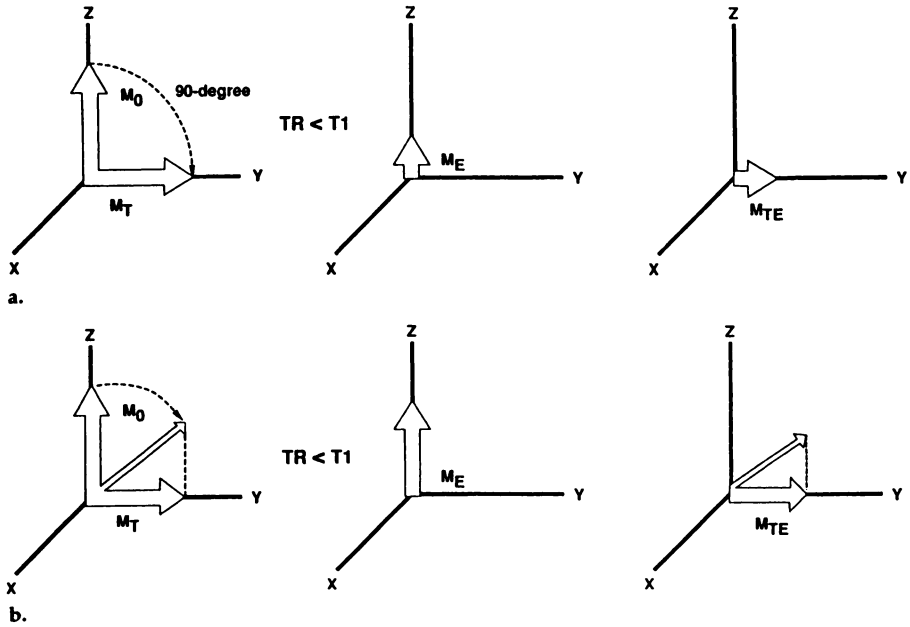

Figure 2. Schematics show how a partial flip can provide greater signal than a 90° flip. **(a)** 90° flip sequence. The first excitation places a large vector of full magnetization (M_0) on the signal-producing plane (M_T). For TRs shorter than T1, the equilibrium magnetization (M_E) after many excitations is small; thus, the transverse signal-producing vector (M_{TE}) is also small. **(b)** 45° partial flip sequence. The initial excitation projects a smaller vector in the transverse plane (M_T), but recovery of magnetization is faster (M_E) so that a larger transverse magnetization (M_{TE}) is achieved after the initial excitation.

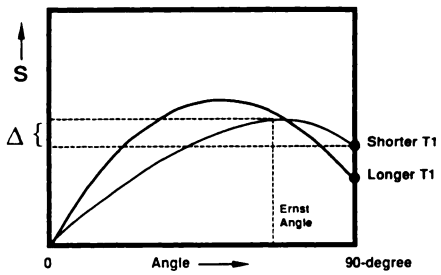

Figure 3. Graph of equation (1). As the flip angle is decreased from 90°, the signal increases up to a maximum at the Ernst angle and then decreases to zero at 0° flip angle. The longer the T1, the larger the increase (Δ) and the smaller the angle at which the peak signal occurs. Therefore, the relative signal levels can reverse from those at 90°. T2 and N(H) only determine the starting levels at 90°, but the reversal is a T1 effect only and can happen even for TEs of 0.

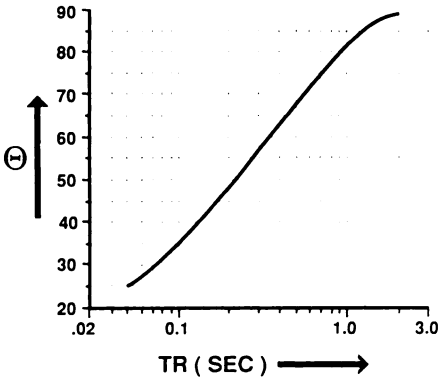

Figure 4. Graph shows the Ernst angle (maximum signal angle) as a function of TR for T1s of 0.5 seconds. A longer T1 results in a smaller Ernst angle at the same TR.

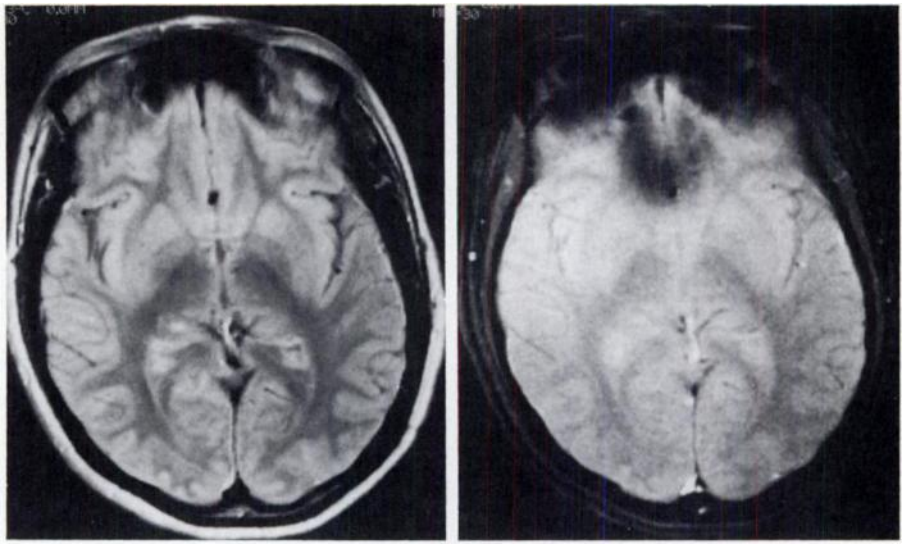

a. **b.**

Figure 5. Example of magnetic susceptibility artifact. **(a)** Spin-echo image obtained at 0.35 T and 2,000/30 (TR msec/TE msec). **(b)** Partial flip image obtained at 0.35 T, 500/30, θ 30°. Artifactual loss of signal in the frontal lobes is seen on **b** due to the enhanced detection of magnetic susceptibility effects by means of gradient echoes. This artifact occurs at interfaces between soft tissues and air-containing spaces such as the nasopharynx, sinuses, and mastoids and will preclude the use of partial flip imaging with gradient reversal as a screening sequence for central nervous system disease.

nique becomes essentially equivalent to that of two-dimensional multisection imaging (6).

If the Ernst angle is used in imaging a tissue of interest, it is possible to increase S/N. More important, if the flip angle is changed (generally to smaller values than the Ernst angle), it is possible to manipulate contrast so that short TRs can be used to obtain images that have the appearance of conventional, long TR images. To see how this happens, let us refer again to Figure 3 and consider the relative changes for the two tissues, one with longer T1 and most likely with greater T2 and N(H). These two tissues may be similar to gray matter and multiple sclerosis lesions, which are difficult to differentiate with short TR procedures: Although the lesions would otherwise have low signal intensity due to their longer T1, the compensating effects of T2 and N(H) nearly cancel signal differences between them and gray matter. For a 90° flip let us say that the lesion is just slightly lower in signal intensity than gray matter. As the flip angle decreases, both tissues start to show a signal increase, but, from equations (2) and (3), the lesions will peak at a smaller angle, and the percentage of increase in signal will be greater. The net effect is that the lesions will increase in intensity. These effects are due to T1 alone. TE (and T2) affect only the starting point at 90°, but the reversal of signal intensity is due to T1 and flip angle. The phenomenon described would occur even for TEs of 0, that is, no T2 effects at all. For those who insist in using the inaccurate T1- and T2-weighted terminology, this phenomenon should add further confusion to that already generated by such vernacular (7). In these terms, what we have described is a short TR sequence (T1-weighted) generating a T2-weighted image through T1 effects only.

GRADIENT REVERSALS

A spin echo is generated as a result of a time reversal experiment. When radio frequency (RF) is used, the 180° refocusing pulse "turns the system around." Those nuclei that are precessing faster, and whose phase (direction of the transverse magnetization vector) is ahead of the mean vector, are now behind. As they continue to precess faster, rather than getting further away from the mean, they catch up with it. Partial flip imaging can in principle be performed with RF refocusing pulses. There is one subtlety. For a single-echo procedure the angle needs to be $180° - \theta$ rather than θ, and for a double-echo procedure it is θ (8). There is a practical problem with this approach, due to imperfect section profiles for the 180° RF pulse. Poor profiles affect contrast in conventional imaging (9), but these effects can be overcome by means of careful shaping (10). These square profiles, although adequate for 90° imaging, degrade unacceptably for small angles, so that the flip angle is varying across the section. It is worth emphasizing that this effect is not fundamental and that, conceptually, an RF pulse can be designed to provide a good section profile for partial flip imaging. Nevertheless, another type of time reversal experiment can be used for generating a readout echo: The magnetization vector is "turned around" or refocused by reversing the readout gradient. This is a very simple process and was used in some early MR imagers but was abandoned for reasons described below. Because gradient reversals are nonselective, the profile of the section is that of the 90° pulse, which is more uniform than the 180° pulse. The nonselectivity of the gradient reversal may lead to the mistaken assumption that it could be used only in a single-section mode, which is not the case. Multisection gradient reversal sequences can be implemented.

Why were gradient reversals abandoned in favor of 180° RF pulses?

The major problem is that gradient reversals are sensitive to background field inhomogeneities. The 180° RF pulse eliminates the effect of background field at the center of the echo; however, in gradient reversal imaging, the effects of inhomogeneities progressively accumulate. These inhomogeneities are not just those resulting from the magnet and its site, but those produced by susceptibility changes in the body in the vicinity of air cavities (sinuses, mastoids, bowel) and those of ferromagnetic implants (Fig. 5). The effects of inhomogeneities not only affect certain areas of the image, but make it difficult to obtain adequate second echoes or very late echoes, except at very low field strengths (the important parameter for imaging is the inhomogeneity in gauss, or the product of the parts per million inhomogeneity times the field strength).

Another problem introduced by gradient reversal refocusing is that the phases of water and fat signals are not brought into coherence, which would occur with an RF refocusing pulse. As TE elapses the signals get further out of phase until they reach 180° phase offset and they cancel fully. As TE elapses further, the signals come back into phase and they add, and this process repeats. At a field strength of 0.35 T the signals are in phase at a TE of 20 msec and fully out of phase at TEs of 10 and 30 msec. The value of TE that brings signals into phase varies in inverse proportion to field strength so that at 1.4 T this value of TE would be 5 msec. This short TE is hard to achieve, and trying to operate at an attainable TE forces the operation to use the second or third echo in a phase cycle. Any small errors in choosing the needed time point will make effective imaging difficult. The effect of water and fat signal cancellation is distinctive in the image. Low-intensity borders show in the regions where water and fat adjoin. These borders can be used to delineate organs (e.g., the pancreas) (Fig. 6) but can also provide confusing information. In the normal marrow the cancellation results in a loss of signal (Fig. 7). Some marrow tumors have high signal intensity in these images (Fig. 8), but diseases that increase iron in the marrow and result in a loss of signal in conventional images would be masked in out-of-phase imaging. In the fatty liver, out-of-phase images decrease the signal, thereby reducing the contrast with respect to tumor in short TR images. Therefore, the ability to obtain in-phase images (no water and fat signal cancellation) will be essential. Unfortunately, as field strength increases, this becomes difficult, and for practical reasons at high field strengths the images will show effects of water and fat signal cancellation.

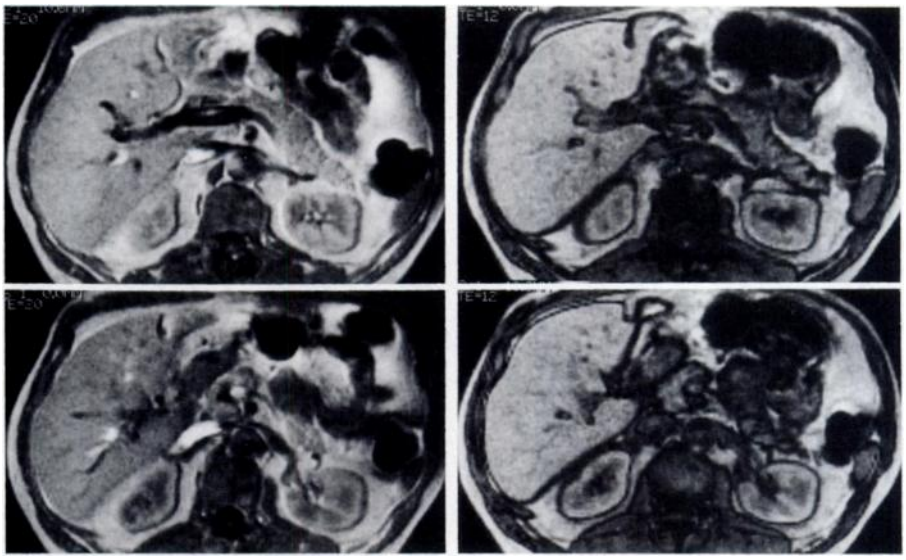

a. b.

Figure 6. Examples of pancreas imaging with partial flip "breath-hold" technique. **(a)** In-phase images obtained at 0.35 T, 250/20, θ 70°. **(b)** Out-of-phase images obtained at 0.35 T, 250/12, θ 70°. Low-intensity outlines around the organs on **b** (TE = 12 msec) are due to water and fat cancellation artifact.

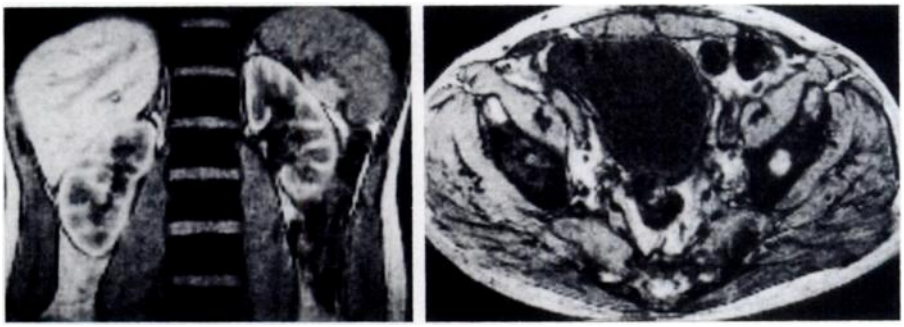

7. 8.

Figures 7, 8. **(7)** Out-of-phase partial flip image of abdomen obtained with breath-hold techniques at 0.35 T, 250/12, θ 70°. The low signal intensity of the bone marrow is due to the out-of-phase cancellation of signal from the water and fat components of the bone marrow. **(8)** Out-of-phase partial flip image of marrow metastases obtained at 0.35 T, 250/12, θ 70°. The bone marrow metastases are easily seen as high-signal-intensity areas because the normal marrow has low signal due to the out-of-phase cancellation of signal from its normal water and fat components.

There is one compensating advantage associated with the use of gradient reversals and partial flip excitations that is quite important at high field strengths. Compared with a 90° flip, a partial flip uses $(\theta/90)^2$ of the power. Thus, for a 45° flip, the excitation power goes down by a factor of four. Even more drastic, the use of gradient reversals saves even more power because the RF refocusing pulse requires four times more power than does a 90° excitation pulse. Gradient reversals require no RF power at all. Therefore, a 45° partial flip with gradient reversals uses one-twentieth the power of a conventional spin-echo sequence with the same TR. This permits rapid imaging techniques to be used at high field strengths, where the power deposition of RF refocusing pulses would otherwise make power deposition excessive. This effect alone assures a role for these techniques in high-field-strength body imaging.

PREDICTION OF THE PARTIAL FLIP PROCESS

The introduction of yet another imaging parameter adds a further degree of complexity to the choice of imaging sequences. For any one TE,

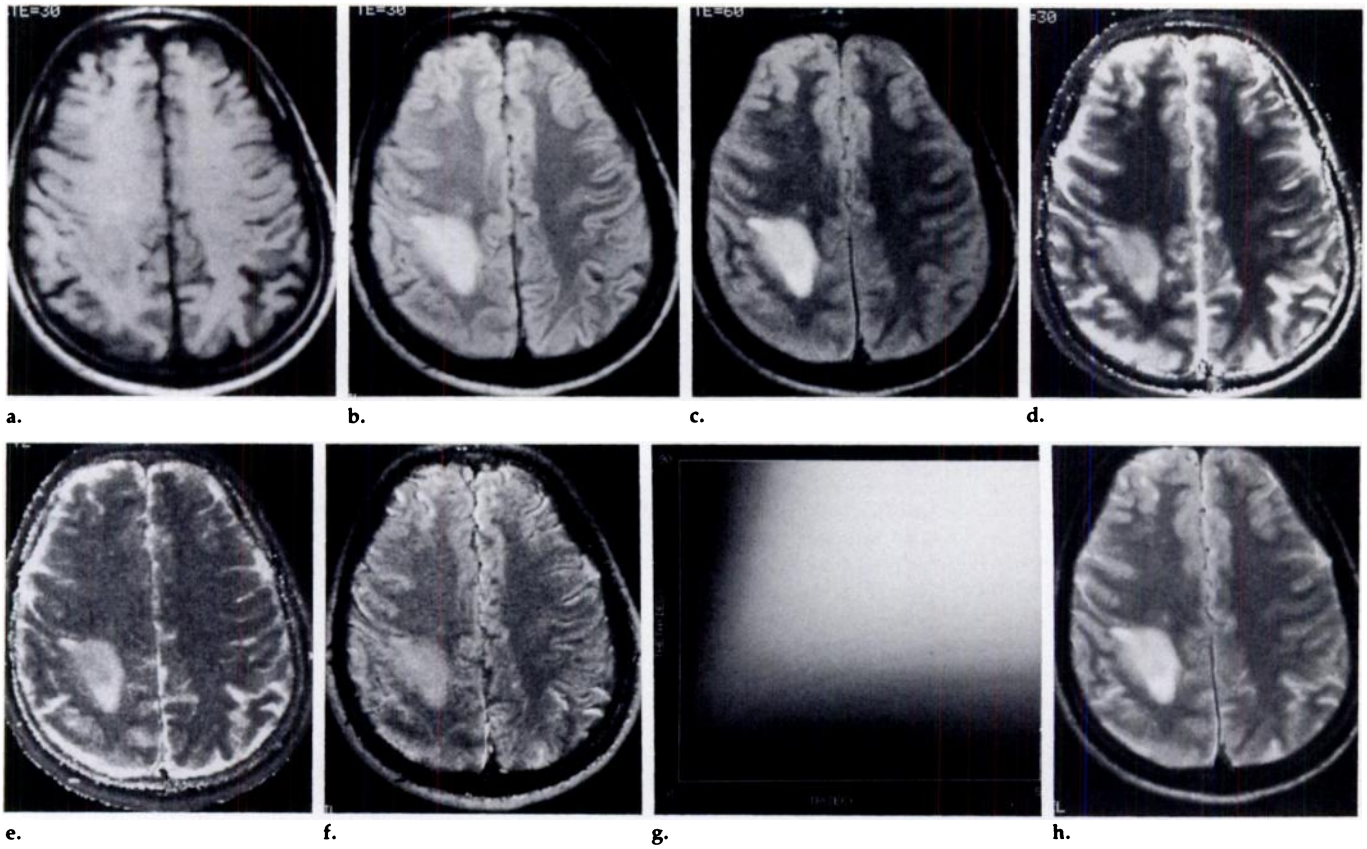

Figure 9. MR imaging sequence demonstrates process of predicting the behavior of partial flip angle imaging. **(a)** Spin-echo 500/30 image. **(b)** Spin-echo 2,000/30 image. **(c)** Spin-echo 2,000/60 image. **(d)** T1 image in which signal intensity is proportional to T1. **(e)** T2 image in which signal intensity is proportional to T2. **(f)** N(H) image in which signal intensity is proportional to N(H). **(g)** Partial flip contrast map of signal differences between the lesion (glioblastoma multiforme) and white matter at a TE of 60 msec. **(h)** Predicted partial flip image (500/60, θ 30°). A conventional contiguous multisection procedure consisting of a short TR image **(a)** and long TR, double-echo images **(b, c)** is used to generate T1, T2, and N(H) images **(d, e, f).** From these, a signal difference map **(g)** is generated for a TE of interest (in this case, 60 msec). The map shows the signal differences between the tumor and white matter as function of TR (horizontal axis) and θ (vertical axis). The largest signal difference is denoted by the highest intensities in the map. From the map, a TR, θ combination is chosen and used to generate a partial flip image **(h)** on a pixel-by-pixel basis based on the T1, T2, and N(H) values of the pixels.

the TR, θ space would have to be sampled in order to characterize a partial flip sequence used to evaluate a particular disease. This is a task that for practical reasons is beyond even a research institution. Fortunately, a library of patient data acquired with appropriate TR/TE combinations can be used to calculate T1, T2, and N(H) images. From these, maps of signal differences for various TR, θ combinations can be computed for particular TE values, and partial flip images can be computed for interesting points in these maps. This process is illustrated in Figure 9. On the basis of such work, we predicted contrast and S/N performance for various partial flip sequences (8), predictions that were then tested and found to agree with experimental data (11) (Fig. 10). The value of being able to do sequence evaluations analytically cannot be overemphasized, since it provides not only an understanding of the process, but also saves a great deal of trial-and-error imaging time.

HISTORICAL DEVELOPMENT

Ernst and Anderson first applied partial flip angle excitation to Fourier transform MR spectroscopy (4). This allowed them to reduce the time of the experiments, and because the pulse repetition interval was relatively short, they found that smaller flip angles improved the S/N. They introduced the familiar relation of equation (1).

In a 1983 patent application, Wehrli proposed applying flip angles of less than 90° to MR imaging in order to reduce acquisition time while maintaining as much of the signal as possible (12). There are several notable aspects to Wehrli's proposal. First, he proposed the use of 180° RF pulses to refocus the magnetization and produce a spin echo. The initial excitation pulse is selective, that is, it excites only the desired section, while the 180° pulses are nonselective. As we saw above, the poor section profile of selective 180° pulses reduces the signal enhancement that would be expected as flip angle is reduced. Therefore, the proposal is for nonselective pulses, which negates multisection acquisition. A second feature of Wehrli's sequence is that even though only one echo is acquired, a second 180° pulse is used after the echo. This is needed, as shown by Mills et al. (8), so that signal will enhance for flip angles less than 90°. If only one 180° pulse is used, then we predict by means of the Bloch equations that signal will enhance if flip angles larger than 90° are used, thus avoiding the second 180° pulse.

In a separate patent application in 1983, Crooks showed that T1 images can be calculated if two images are acquired at the same TR but with two different flip angles (13). T1 images can thus be calculated in a shorter time than is required when the more customary method of image acquisition at two different TRs is used (11).

Fast imaging techniques with par-

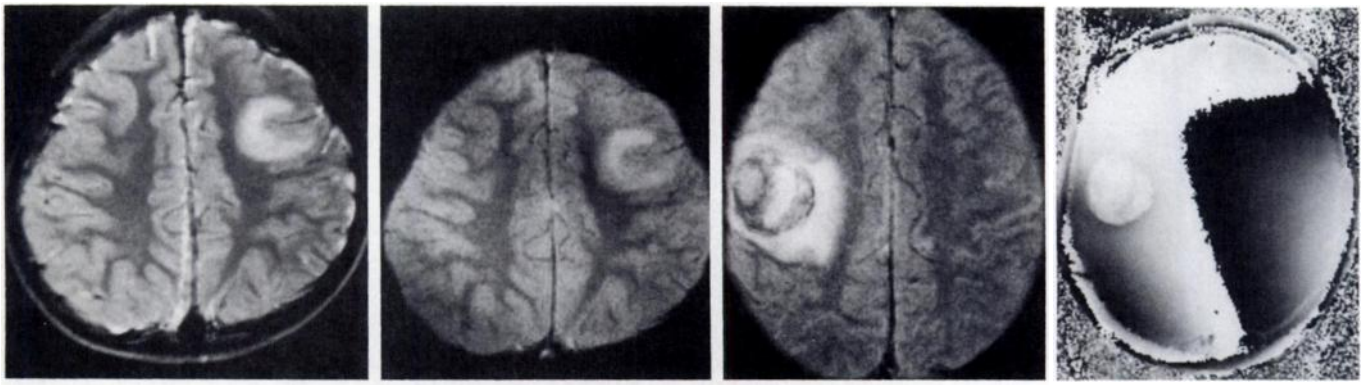

10a. 10b. 11a. 11b.

Figures 10, 11. **(10)** Predicted versus actual partial flip image. **(10a)** Predicted partial flip image obtained at 0.35 T, 500/30, θ 30°. **(10b)** Acquired image. Because the predicted image is based on conventional spin-echo data acquired over approximately 22 minutes, the S/N of the predicted image is better than that of the acquired image, which was obtained in approximately 2 minutes. The S/N for partial flip imaging relative to conventional imaging is also predictable (11). The lesion proved to be a tuberculoma. **(11)** Hemorrhagic metastasis. **(11a)** Partial flip image obtained at 0.35 T, 500/30, θ 30° shows a complex right hemispheric lesion with some low-intensity areas suggestive of hemorrhage. **(11b)** The phase map of **11a** demonstrates a sharp focal variation in phase that allows for a definite diagnosis of hemorrhage within the lesion.

tial flip angles have been introduced relatively recently, accompanied by a confusing array of acronyms. Since the introduction of the FLASH (fast low angle shot) sequence (14), a number of groups have introduced variants of their own such as FFE (fast field echoes) (15), GRASS (gradient recalled acquisition in the steady state) (16), FAST (Fourier acquired steady-state technique) (17), FISP (fast imaging with steady precession) (18), and techniques that simply go by the name partial flip (11). In most cases, it appears as if the desire for a cute or catchy acronym drives the choice of words used to describe the technique. A key feature of all these various techniques is the use of partial flip angles, short TRs, and the lack of 180° RF pulses in spin-echo refocusing. Instead, a gradient reversal technique is used to refocus the echo.

The literature is not consistent about the appropriate nomenclature for this type of echo. Some authors refer to it as a spin echo, while others believe that this term should be reserved for echoes produced by means of 180° pulses. Other common terms are gradient echo, gradient reversal echo, field echo, gradient recalled echo, and free induction decay. As with most endeavors in life, simplicity should be encouraged. Clearly, three words are not needed to characterize the echo: For instance, use of recalled or refocused is redundant in describing a gradient echo. Field echo is ambiguous, and spin echo applies both to RF and gradient refocusing. It would seem that gradient echo (7) is fully explanatory and unambiguous enough for the MR imaging field. When talking about sequences themselves, it would appear that they can be called RF refocused and gradient refocused techniques.

Although there are important differences between gradient and RF refocusing, once the time domain data are received, the reconstruction methods are the same in all cases. Short TR imaging introduces a complication not found when the TR is long. The transverse magnetization decays with a time constant T2. When TR exceeds T2, the transverse component decays between excitations, but this is not the case when TR is short. The fast partial flip sequences listed above differ in how they deal with this issue. By proper arrangement of the symmetry of the gradient pulses and choice of flip angle, one can form two images, each with a very different contrast appearance. This is evident in comparing the contrast in images obtained with the FLASH and FISP techniques. The FLASH image is nominally independent of T2, whereas the FISP image is produced with a steady-state free precessional signal and depends explicitly on the ratio of relaxation times T2/T1. One potential problem with steady-state free precession is that it can be extremely sensitive to motion. For example, early work by Holland et al. showed that the cerebrospinal fluid can become low in intensity with steady-state free precession, which was interpreted as evidence for cerebrospinal fluid pulsations (19).

Although for the most part the early motivation for the use of partial flip angles was a desire for more signal intensity at short TRs, some investigators recognized that variation of flip angle could result in a change in contrast. Mills et al. (8) showed that soft-tissue contrast similar to that obtained with long TR imaging could be obtained at short TRs by use of a partial flip angle. It is this latter characteristic of partial flip MR imaging that is likely to be the most important in the long term.

CLINICAL APPLICATIONS

A review of the clinical applications and operating mode of a recently introduced technique is by definition incomplete as it is written. Therefore, in this review we will mention some uses and limitations as they are now understood and present some near-term projections for future uses.

In the brain, the primary role of partial flip MR imaging will be to produce more sensitive and specific information about the presence of intracranial hemorrhage. Winkler et al. (20) have shown that the decrease in signal intensity in hemorrhagic lesions is far greater with partial flip imaging than with spin-echo imaging because of the enhanced detection of magnetic susceptibility produced by the gradient echoes employed in a partial flip sequence. This superiority can be augmented if phase images of the partial flip sequence are also viewed (20)[2] (Fig. 11). Intracranial hemorrhages demonstrate a sharp focal variation in phase with the partial flip procedure due to

[2] Young IR. Phase-dependent imaging techniques offer a new direction in MR. Diagn Imaging 1987; 9:119.

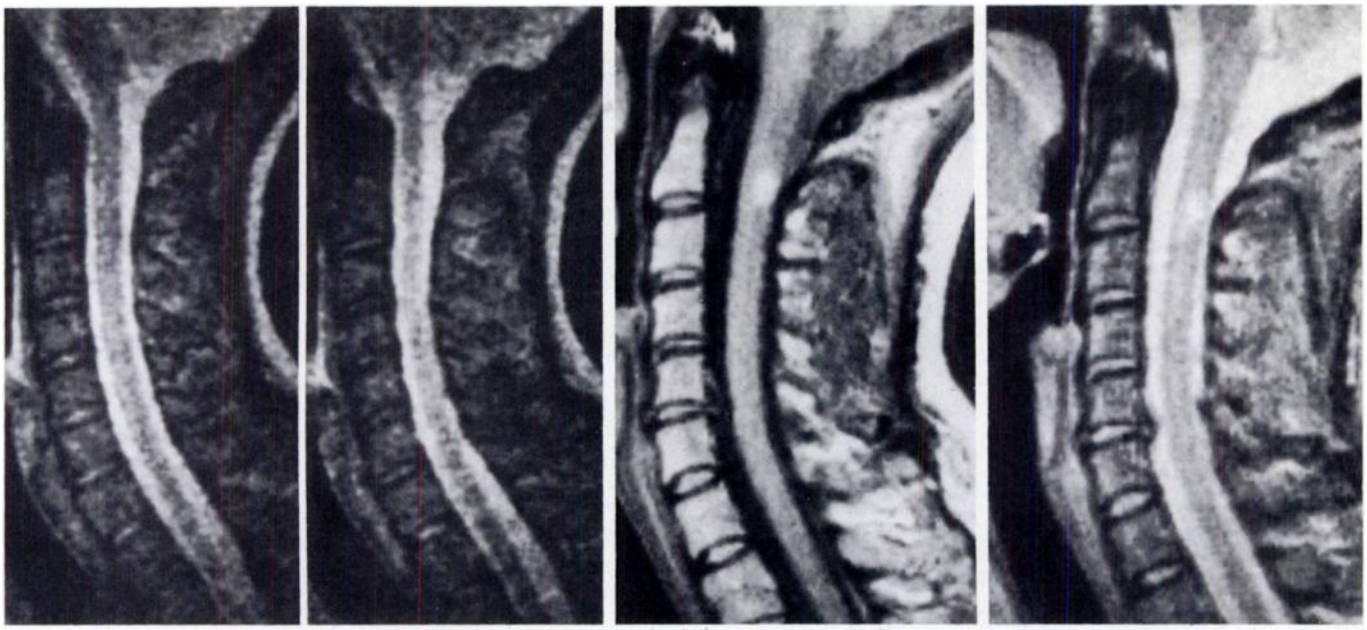

12. 13a. 13b.

Figures 12, 13. **(12)** MR myelogram obtained at 0.05 T with partial flip technique (1,200/40, θ 30°). The use of a reduced flip angle produces high-intensity cerebrospinal fluid for a myelographic effect that is very useful in the assessment of compromise of the subarachnoid space from degenerative causes. **(13)** Cervical disk herniation and multiple sclerosis plaque. **(13a)** Spin-echo image obtained at 0.35 T, 1,500/40. **(13b)** Partial flip image obtained at 0.35 T, 1,000/20, θ 28°. Both studies demonstrate a central C5-6 disk herniation, but the contrast for the spinal cord lesion is superior on **13a.**

enhanced detection of magnetic susceptibility. This increased detection of intracranial hemorrhage is seen at both medium and high magnetic field strengths (20, 21).

Unfortunately, the increased magnetic susceptibility seen with partial flip imaging will preclude its effective use in certain parts of the brain. At interfaces between air and soft tissue (i.e., near the sinuses, mastoids, and nasopharynx), areas of artifactually diminished signal intensity are observed (Fig. 5). The appearance of this artifact is influenced by volume averaging between air and soft-tissue regions. For example, the temporal lobes are better examined in a coronal rather than an axial plane to minimize volume averaging with the mastoids. If the entire brain were to be adequately studied with partial flip procedures, multiplanar imaging would be needed to displace the location of the artifact to different parts of the brain on different views. Although a properly designed partial flip procedure can result in contrast as good as that achieved with a properly designed spin-echo procedure, the presence of these artifacts will mean that the former will be relegated to an adjunctive rather than a screening role (20, 21).

Partial flip imaging of the brain also appears to have nonhemorrhagic applications. Drayer et al. have presented work demonstrating that the enhanced detection of magnetic susceptibility further allows for the identification of brain iron within normal structures, such as the globus pallidus, red nucleus, and substantia nigra, and may allow better identification of certain metabolic disease states and better characterization of meningiomas (22). They have also suggested that partial flip imaging may be useful in examining cerebrospinal fluid flow phenomena, vascular flow phenomena, and intracranial mineralization.

In the spine, the primary role of partial flip imaging will be in enabling the rapid production of MR myelograms (Fig. 12). With partial flip imaging, a short TR combined with a reduced flip angle can be used to produce high-intensity cerebrospinal fluid with significantly reduced artifact from pulsatile flow, compared with that resulting from a much longer TR spin-echo procedure. Mills and Winkler (23) and Hedberg et al. (24) have demonstrated, at medium and high field strengths respectively, that partial flip MR myelography is superior to conventional spin-echo imaging in depicting compromise of cervical subarachnoid space from degenerative or disk disease. The availability of partial flip MR myelography may obviate the need, suggested by Rubin et al. (25), for cardiac gating in order to produce the myelographic effect at high field strengths and avoid cerebrospinal fluid flow artifacts.

Unfortunately, Mills and Winkler (23) and Hedberg et al. (24) independently found that partial flip MR myelography cannot fully replace conventional spin-echo procedures. Short TR/short TE images better depict spinal cord and medullocervical junction anatomy and remain necessary to demonstrate disease metastatic to the spine. Long TR/intermediate-to-long TE sequences remain necessary to best detect spinal cord abnormalities such as myelomalacia, myelitis, and multiple sclerosis. Although a partial flip MR myelographic procedure can be designed to show spinal cord lesions, the contrast for the lesion will not be as good as that achieved with a properly designed spin-echo procedure (Fig. 13). In addition, the difficulty of mistaking a spinal cord lesion for volume-averaged high-intensity cerebrospinal fluid is much less of a problem with the latter technique because the lesions can be made to increase in signal intensity (first echo) before the cerebrospinal fluid (second echo) does. It is anticipated that partial flip MR myelography will have an important role in the diagnosis of degenerative and disk disease in the thoracic spine where pulsatile cerebrospinal fluid motion can be a problem. In the lumbar spine, where cerebrospinal fluid flow is less trouble-

some, partial flip MR myelography will have a less dramatic impact on diagnostic quality but may well prove useful for reducing imaging times.

In the abdomen, the primary role of partial flip imaging will be in the performance of "breath-hold" sequences (i.e., those in which subjects momentarily suspend respiration) to eliminate respiratory motion artifacts (26, 27).[3] For a breath-hold procedure the TR must be short (<250 msec) to accomplish the study quickly (<32 seconds). For such a short TR, S/N in the upper abdomen can be improved by decreasing the flip angle to slightly less than 90° (11). However, several difficulties arise with partial flip breath-hold procedures. First, flow artifacts in the phase-encoded direction are increased, which necessitates the introduction of presaturation pulses, which in turn limit the number of sections obtained in one breath-hold sequence (28). Second, the TE must be carefully chosen to avoid obtaining the water and fat phase cancellation artifact, which produces low-intensity outlines around organs (Fig. 6). Also, the increased magnetic susceptibility due to the gradient echoes can have the unexpected consequence of reducing the contrast of hepatic lesions (Fig. 14). At this time, much needs to be learned about the consequences on contrast of operating in versus out of phase and about the impact of magnetic susceptibility on contrast in the liver in order to recommend these protocols for routine clinical use. For the above reasons, they may eventually prove less useful than their higher contrast, lower S/N, lower artifact counterparts, obtained by means of conventional spin-echo breath-hold procedures. At this time, the partial flip breath-hold procedure in the upper abdomen remains an adjunctive sequence to the combination of a multiacquisition short TR/short TE procedure and a long TR/long TE procedure.

In the heart and vascular system, partial flip imaging has opened new avenues of exploration in the areas of cine cardiac MR imaging, as well as MR angiography. Partial flip cine cardiac MR imaging can produce images in which the blood has increased signal intensity and thus allows better appreciation of flow patterns. Preliminary research by Utz et al. (29) and Sechtem et al. (30), among others, has shown that partial flip cine cardiac MR imaging can yield functional information such as stroke volume, ejection fraction, and regional wall motion and contractility. Abnormally contracting infarcted or aneurysmal regions have been detected with this technique. In addition, cardiac valve motion and flow turbulence from stenotic or regurgitant lesions can be characterized (31–33). The partial flip cine cardiac MR imaging techniques have been effectively applied at field strengths of 0.05–1.5 T (Fig. 15). The main question is whether the technique will provide additional cost-effective information compared with that available from the existing noninvasive

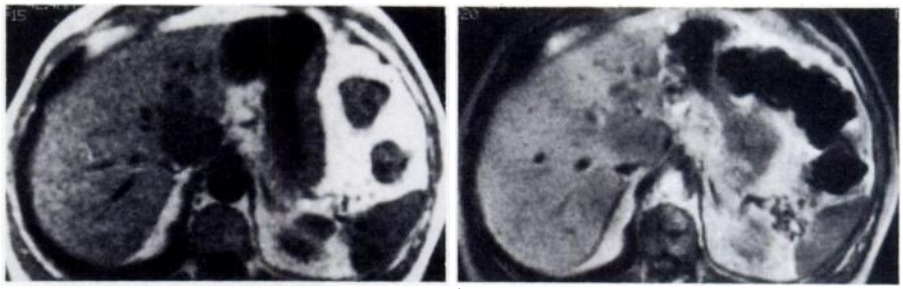

a. b.

Figure 14. Caudate hepatic metastasis. **(a)** Spin-echo image obtained with breath-hold technique at 0.35 T, 250/15. **(b)** Partial flip image obtained with breath-hold technique at 0.35 T, 250/20, θ 70°. Even though the partial flip procedure produces superior S/N, the lesion is better seen on **a** due to superior contrast. Much remains to be learned about the application of partial flip technology to hepatic imaging.

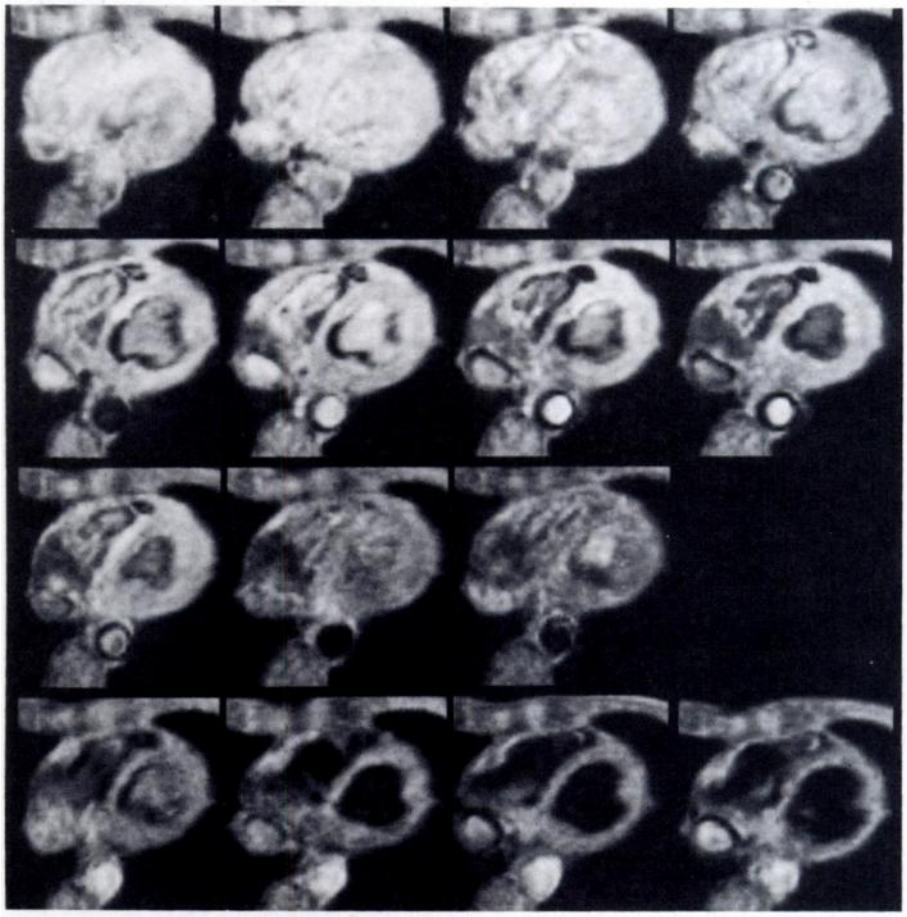

Figure 15. Sequence of cine cardiac MR images obtained at 0.05 T. Images from eight cardiac levels with 16 time points per beat, 30 msec apart, are obtained in 20 minutes and are displayed in a cine mode. Such cine MR images provide both anatomic and functional information.

[3] Winkler ML. Better contrast gives MR an edge in upper abdomen. Diagn Imaging 1987; 9:90–95.

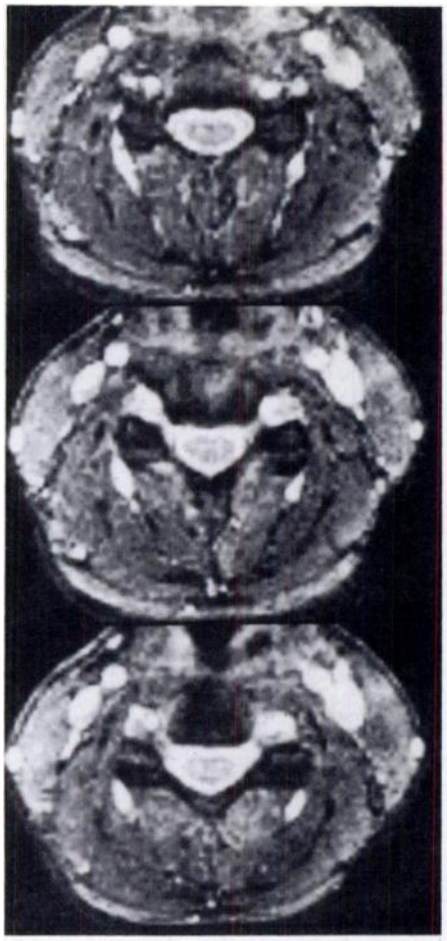

Figure 16. Three-dimensional partial flip images of the cervical spine obtained at 0.35 T, 60/20, θ 7°. Thirty-two contiguous 2-mm sections are acquired in 16 minutes. The highly reduced flip angle yields a myelographic effort for superb delineation of the subarachnoid space around the cord and nerve roots.

modalities of echocardiography and nuclear medicine.

Gradient reversal procedures are also helpful in MR angiography, during which projected views of vessels are obtained (34, 35). However, projection techniques do not provide the detailed information available in conventional spin-echo views obtained transverse to the vessel (36, 37). Although many problems remain to be solved, such as the apparent disappearance of certain portions of a vessel (38), MR angiographic techniques may prove of value in specific applications or in providing localization views for transverse imaging.

An interesting role for partial flip MR imaging will be to produce extremely thin sections with three-dimensional Fourier transform techniques. This topic is reviewed in detail by Carlson et al. (6). Partial flip imaging offers the best opportunity for three-dimensional Fourier transform applications because good S/N can be maintained with an extremely short TR by means of significantly reducing the flip angle. Three-dimensional techniques also offer the benefit of overcoming the magnetic susceptibility artifacts seen with two-dimensional techniques. Dramatic thin-section three-dimensional partial flip images have been shown by many groups in anatomic locations such as the cervical spine (Fig. 16) and knee. However, for a fixed imaging time with partial flips, the three-dimensional imaging technique has no advantage in S/N compared with that achieved in two-dimensional acquisitions, and it has reduced flexibility in sequence design.

CONCLUSION

The clinical radiologist can think of partial flip MR imaging as a time-saving technique in which TR and flip angle are manipulated to yield a desired contrast. Partial flip imaging offers the clinical radiologist a powerful tool for the detection of intracranial hemorrhage and for the production of MR myelograms. It also opens new horizons for brain, abdominal, cardiac, vascular, and thin-section three-dimensional imaging. In most applications, however, it will supplement rather than replace conventional spin-echo procedures. ■

References

1. Ortendahl DA, Hylton NM, Kaufman L, et al. Analytical tools for magnetic resonance imaging. Radiology 1984; 153:479–488.
2. Ortendahl DA, Hylton NM, Kaufman L, Crooks LE. Signal to noise in derived NMR images. J Magn Reson Med 1984; 1:316–338.
3. Ortendahl DA, Posin JP, Hylton NM, Mills CM. Optimal visualization of the cerebrospinal fluid in MRI. AJNR 1986; 7:403–407.
4. Ernst RR, Anderson WA. Application of Fourier transform spectroscopy to magnetic resonance. Rev Sci Instr 1966; 37:93–102.
5. Kaufman L, Crooks LE. Realistic expectations for the near term development of clinical NMR imaging. IEEE Trans Med Imaging 1983; MI2:57–65.
6. Carlson JC, Crooks LE, Ortendahl DA, Kramer DM, Kaufman L. Signal-to-noise ratio and section thickness in two-dimensional versus three-dimensional Fourier transform MR imaging. Radiology 1988; 166:266–270.
7. Axel L. Revised glossary of MR terms. Radiology 1987; 162:874.
8. Mills TC, Ortendahl DA, Hylton NM. Investigation of partial flip angle MR imaging. IEEE Trans Nucl Sci 1986; 33:496–500.
9. Kneeland JB, Shimakawa A, Wehrli FW. Effect of intersection spacing on MR image contrast and study time. Radiology 1986; 158:819–822.
10. Feinberg DA, Crooks LE, Hoenninger JC, et al. Contiguous thin multi-section MR imaging by two-dimensional Fourier transform techniques. Radiology 1986; 158:811–817.
11. Mills TC, Ortendahl DA, Hylton NM, Crooks LE, Carlson JW, Kaufman L. Partial flip angle MR imaging. Radiology 1987; 162:531–539.
12. Wehrli F. Method for rapid acquisition of NMR data. Washington, D.C.: U.S. Patent Office, May 6, 1986. Patent no. 4,587,489, filed 1983.
13. Crooks LE. Apparatus and method for T1 NMR imaging using spin echo NMR responses elicited by initial excitation pulses of differing nutation values. Washington, D.C.: U.S. Patent Office, October 6, 1987. Patent no. 4,698,593, filed 1983.
14. Haase A, Frahm J, Matthaei D, Hanicke W, Merboldt KD. Flash imaging: rapid NMR imaging using low flip angle pulses. J Magn Reson 1986; 67:258–266.
15. Van der Muelen P, Grown JP, Cuppen JJM. Very fast MR imaging by field echoes and small angle excitation. Magn Reson Imaging 1985; 3:297–299.
16. Utz JA, Herfkens RJ, Glover G, Pelc L. Three second clinical NMR images using a gradient recalled acquisition in a steady state mode (GRASS) (abstr.). Magn Reson Imaging 1986; 4:106.
17. Gyngell ML, Palmer ND, Eastwood LM. The application of steady-state free precession (SFP) in 2DFT MR imaging (abstr.). In: Book of abstracts: Society of Magnetic Resonance in Medicine 1986. Berkeley, Calif.: Society of Magnetic Resonance in Medicine, 1986; 666–697.
18. Oppelt A, Graumann R, Barfud H, Fischer H. FISP: a new fast MRI sequence. Electromedica 1986; 54:15–17.
19. Holland GN, Hawkes RC, Moore WS. NMR tomography of the brain: coronal and sagittal sections. J Comput Assist Tomogr 1980; 4:429–433.
20. Winkler ML, Olsen WL, Mills TC, Kaufman L. Hemorrhagic and nonhemorrhagic brain lesions: evaluation with 0.35-T fast MR imaging. Radiology 1987; 165:203–207.
21. Drayer BP. Neurological applications of variable flip angles in MR imaging. Presented at the Fourth Annual MRI National Symposium, Las Vegas, May 4–8, 1987.
22. Drayer BP, Bird R, Hodak J, Flom RA. Limited flip angle MR Imaging: non-hemorrhagic applications. Presented at the 25th Annual Meeting of the American Society of Neuroradiology, New York, May 10–15, 1987.
23. Mills TC, Winkler ML. Rapid MR myelography: clinical results at .35 Tesla. (abstr.). In: Book of abstracts: Society of Magnetic Resonance in Medicine 1987. Berkeley, Calif.: Society of Magnetic Resonance in Medicine, 1987.
24. Hedberg MC, Drayer BP, Flom RA, et al. Gradient echo (GRASS) MR imaging in cervical radiculopathy (forthcoming).
25. Rubin JB, Enzmann DR, Wright A. CSF-gated MR imaging of the spine: theory and clinical implementation. Radiology 1987; 163:784–792.
26. Edelman RR, Hahn PF, Buxton R, et al. Rapid MR imaging with suspended respiration: clinical application in the liver. Radiology 1986; 161:125–131.
27. Utz JA, Herfkens RJ, Johnson CD, et al. Two-second MR images: comparison with spin echo images in 29 patients. AJR 1987; 148:629–633.

28. Ehman RL, Felmlee JP. Spatial presaturation: a method for suppressing flow artifacts and improving depiction of vascular anatomy in MR imaging. Radiology 1987; 164:559–564.
29. Utz JA, Herfkens RJ, Heinsimer JA, et al. Cine MR determination of left ventricular ejection fraction. AJR 1987; 149:839–843.
30. Sechtem U, Pflugfelder PW, White RD, et al. Cine MR imaging: potential for the evaluation of cardiovascular function. AJR 1987; 148:239–246.
31. Fisher MR, Rogers LF. Cardiac left ventricular ejection fraction calculation using field echoes in MR imaging. Magn Reson Imaging 1987; 5(1):143.
32. Pflugfelder P, Sechtem U, White R, Higgins CB. Noninvasive measurement of regurgitant fraction in patients with mitral or aortic regurgitation by cine MRI. Magn Reson Imaging 1987; 5(1):141.
33. Underwood JR, Firmin DN, Mohaiddin RH, et al. Cine magnetic resonance imaging of intracardiac flow patterns. Magn Reson Imaging 1987; 5(1):141.
34. Dumoulin CL, Hart HR Jr. Magnetic resonance angiography. Radiology 1986; 161:717–720.
35. Nishimura DG, Macovski A, Pauly JM, Conolly SM. MR angiography by selective inversion recovery. Magn Reson Med 1987; 4:193–202.
36. Valk PE, Hale JD, Kaufman L, Crooks LE, Higgins CB. MR imaging of the aorta with three-dimensional vessel reconstruction: validation by angiography. Radiology 1985; 157:721–725.
37. von Schulthess GK, Augustiny N. Calculation of T2 values versus phase imaging for the distinction between flow and thrombus in MR imaging. Radiology 1987; 164:549–554.
38. Masaryk TJ, Modic MT, Haacke EM, et al. MR angiography of carotid bifurcation with correlations for velocity and acceleration. Presented at the 25th Annual Meeting of the American Society of Neuroradiology, New York, May 10–15, 1987.